

Administration Methodology for a wind/solar Hybrid Energy System

Boualam BENLAHBIB^{1,2}, Noureddine BOUARROUDJ¹, Saad MEKHILEF²

¹Unite de Recherche Appliquee en Energies Renouvelables (URAER), Centre de Developpement des Energies Renouvelables (CDER), 47133 Ghardaia, Algeria

²Power Electronics and Renewable Energy Research Laboratory (PEARL), Department of Electrical Engineering, University of Malaya, 50603 Kuala Lumpur, Malaysia

E-mail: bouallam30@gmail.com

Abstract – A control of a stand-alone hybrid wind solar powered energy framework with battery capacity is presented in this paper. The framework is composed of a wind turbine, photovoltaic panels, a capacity battery unit and a three-phase AC stack. Electronic converters play a critical role in interfacing the various sources with a DC primary link to supply a three-phase stack. The purposes of this set up are to ensure permanent stack supply and coordination between the distinct sources of the framework. The wind turbine and the photovoltaic panel are monitored to operate under extreme conditions. An MPPT controller is employed to extract the available power from the wind and solar powered sources. A speed regulator and a Single Input Fuzzy Logic Controller SIFLC are utilized. An Energy Administration Framework (EAF) based on the battery state of charge is created and updated through Matlab-Simulink to guarantee the consistency of stack supply. A line-to-line AC voltage adjustment based on a PID controller was implemented to supply the RL stack with stable amplitude and frequency.

Keywords – Energy Administration Framework (EAF), Wind energy, Solar energy, Storage, hybrid system, Control, Fuzzy.

I. INTRODUCTION

Variable Nowadays the most exploited renewable energy resources are solar and wind energy. According to ‘Renewables Worldwide Status report (2020) (REN21)’, wind power can be considered as the leading source of renewable power generating capacity in USA and Europe in 2019, and the second biggest power asset in China. Globally, a wind energy capacity of 60 GW was installed, to be added to an existing capacity of around 651 GW. Based on the quality and low cost of the wind power, numerous organizations and private companies are increasingly turning to this kind of power source, and numerous renowned financial specialists have been stressing the steady income it generates [1].

The leading source of added power capacity in 2019 was the solar powered PV in a few markets such as India, Japan, United States, and China. Worldwide, at least 115 GW of solar powered PV capacity was introduced (on-and-off-grid), expanding the capacity by about one-third, to a total of roughly 627 GW [1].

The requirement for an Energy Administration Methodology for a Hybrid Energy System HES unequivocally emerges to screen the energy stream through the power framework. This requirement is not as it were for the HES in separated sites, but it is additionally imperative for the HES associated to an electrical power grid. Among the objectives of this administration procedure is to supply the loads in a consistent way under all conditions, ensure optimal operation of renewable energy sources, protect gear against over-burdens achieve cost optimization, and enhance the robustness of the energy framework.

Moreover, the administration procedures within the HES associated to power networks consist in controlling in controlling the power flow to and from grid and other tallying purposes. The HES disengagement at stack peak moments and the operation in periods characterized by reduced power demand are among the other objectives of the administration procedures [2].

A few administration procedures were proposed in the literature; for instance, a standalone mode HES was proposed in [3] to address the intermittency issue.

The authors assessed three administration procedures of HES in separated location comprising PV / wind / PEMFC (Proton Exchange Membrane Fuel Cells), where the PV and wind are utilized as essential sources, and PEMFC is used as an auxiliary or a reinforcement source. The procedures serve to extend the fuel cell layer and guarantee steady power from the HES to the stack. In [4] the authors assessed the execution of two administration procedures in which they utilized hysteresis band; the HES, which incorporates PV, wind and a capacity framework based on hydrogen was monitored for a period of more than four months. Hysteresis band exhibited high adaptability for FC, Electrolyzer, and battery operations, and reduced the number of start-ups-shutdowns of capacity sources [2].

On the other hand, for HES connected to electrical networks, authors in [5] proposed a consumer-side control administration to coordinate it with the tallying framework. In this set up, a pre-processed tallying framework was actualized and presented with control that acted on user's request. This serves to confine the users to be restrictive with the accessibility of renewable energy on a month-to-month premise. In [6] authors proposed a PV framework associated to the electrical organize for feeding a DC stack from this electrical set up without breaking any excess of control can be infused into the electrical organize with a high quality. The battery voltage was controlled, and the signals that show the state of charge (SOC) or more deep discharge of the battery are produced [2], to choose the working mode of the bidirectional converter (buck or boost).

In this paper, to handle the issue of stream administration in standalone HES, a control framework was proposed and confirmed through Matlab-Simulink based on batteries SoC. This paper is organized as follows: section 2 presents an overview and illustration of the various parts of the HES. The details of the administration methodology of HES proposed in this paper are illustrated in section 3. Results and discussion are given in section 4. The conclusions and future works are given in section 5.

II. EXPLANATION AND MODELLING OF A HYBRID ENERGY SYSTEM

This consider bargains with a hybrid system with three renewable energy sources : wind turbine (WT), photovoltaic (PV) panels and capacity batteries. WT

and PV panels are utilized as essential energy sources, whereas capacity batteries are utilized as auxiliary or reinforcement energy sources. The framework examined here comprises a wind generator of 5 kW, and a PV generator of 5 kW. The common block diagram of a hybrid system is shown in Figure.1.

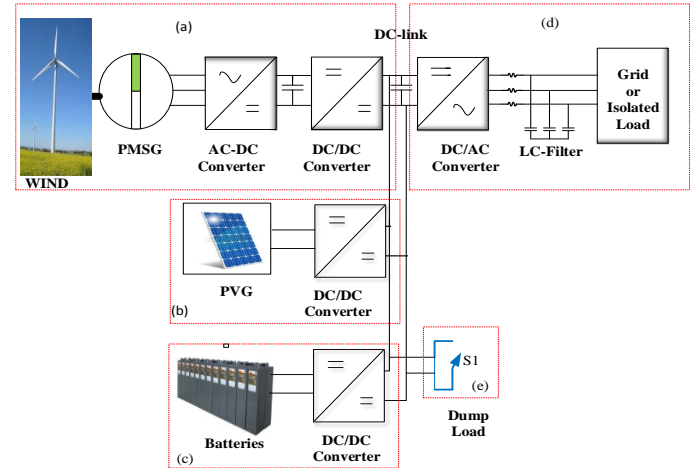


Fig. 1. Structure of the studied Hybrid Energy framework

The examined framework can be separated into four parts:

- a- The WT generator side comprises a PMSG, an uncontrolled bridge diode and a boost DC-DC converter.
- b- The PV generator side contains PV modules and a DC-DC boost converter for MPPT
- c- The stack side includes a three-phase Inverter LC filter, and RL stack, besides, a dump stack is employed to secure the batteries from overcharging.
- d- The storage system side contains a buck-boost DC-DC converter with lead acid battery.

The DC interface voltage is dependent on WT, PV generators control yield and the stack impedance [7], The authors utilized Fractional order PID control approach for the DC-link voltage to overcome unsteady voltage supply [7][8] based on the buck-boost DC-DC converter[10]. The DC-AC converter was controlled using the line-to-line stack yield voltage control based on a PID controller.

A) Wind Generator Modeling

The wind generator utilized in this ponder is made up of a wind turbine, a permanent magnet synchronous generator (PMSG), an uncontrolled rectifier and a Boost converter. The model of each component is displayed as follows :

a. Wind turbine :

The sum of streamlined power P_{aer} collected from the wind turbine (WT), as shown in figure 1 (a), can be expressed by the following formula :

where P_{aer} is the streamlined power (W), ρ is :

$$P_{aer} = C_p \cdot P_v = C_p(\lambda, \beta) \cdot \frac{\rho S V^3}{2} \quad (1)$$

the air density (kg/m^3), V is the wind speed (m/s), S is the cleared region of the turbine (m^2), and C_p is the power coefficient of wind speed characterized according to [10, 11] :

$$C_p(\lambda, \beta) = (0.5 - 0.06167) \sin \left[\frac{\pi(\lambda+0.1)}{18-0.3(\beta-2)} \right] - 0.00184(\lambda-3)(\beta-2) \quad (2)$$

β is a blade pitch angle; λ is speed proportion characterized as follows:

$$\lambda = \frac{\Omega_t R}{V_{wind}} \quad (3)$$

Ω_t is turbine speed, V_{wind} is the wind speed. R is the radius of turbine blades.

The relation between wind power coefficient :

$C_p(\lambda, \beta)$ and a tip speed ratio (λ) when blade pitch-angle $\beta = 2^\circ$ as displayed in Figure.2.

$\beta = 2^\circ$

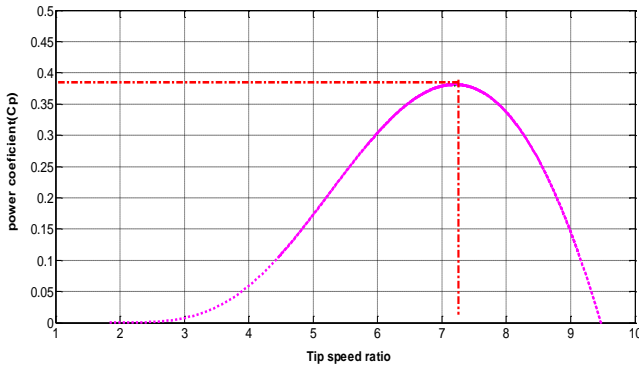


Fig. 2. Power coefficient C_p and tip speed ratio λ characteristics

The streamlined torque is given by :

$$C_{aer} = \frac{P_{aer}}{\Omega_t} = C_p \cdot \frac{\rho S V^3}{2} \cdot \frac{1}{\Omega_t} \quad (4)$$

The most objective of the maximum power Point tracking (MPPT) control in wind turbine is to guarantee the extraction of the maximum available power from the wind. There are distinctive MPPT

control calculations, among them the ideal torque control based on the following equation :

$$P_{opt} = C_p^{opt}(\lambda_{opt}, \beta) \cdot \frac{\rho S V^3}{2} \quad (5)$$

As can be noted, the power coefficient C_p may be a work of λ and β and comes to the greatest at the specific λ denoted λ_{opt} , should be considered in the estimate, with the ideal rotor speed. More points of interest on this type of MPPT control can be found in [10].

b. PMSG Model

The energetic demonstration of PMSG appeared in figure 1 (a) is illustrated in d-q axis rotor outline, in which the q-axis is 90° ahead of the d-axis, with regard to the direction of rotation. The stator voltage of PMSG can be expressed as follows [10, 11] :

$$\begin{cases} -R_s i_{ds} - L_d \frac{di_{ds}}{dt} + \omega L_q i_{qs} = v_{ds} \\ -R_s i_{qs} - L_q \frac{di_{qs}}{dt} + \omega L_d i_{ds} + \omega \cdot \varphi_f = v_{qs} \end{cases} \quad (6)$$

Where : v_{ds} , v_{qs} : d-q axis stator voltage, i_{ds} , i_{qs} : d-q axis stator current, L_d , L_q : d-q axis inductance, R_s : stator resistance, ω : electrical pulsation, φ_f : magnetic flux.

The electromagnetic torque is written as follow :

$$T_{em} = \frac{3}{2} P [(L_q - L_d) \cdot i_{ds} i_{qs} + i_{qs} \varphi_f] \quad (7)$$

where P : pole pairs number.

According to flux axes orientation Eq (7) becomes as follows:

$$T_{em} = \frac{3}{2} P i_{qs} \varphi_f = K \cdot i_{qs} \quad (8)$$

c. Uncontrolled AC-DC Converter

When wind speed changes with time, the PMSG rotational speed changes as well. Consequently, the voltage produced by the PMSG shifts in amplitude and frequency. In this case, the voltage is unacceptable for both clients and electric loads [12]. Subsequently, to prevent such a disturbance, the created voltage is converted to DC voltage and then converted to an AC voltage controllable in amplitude and frequency. In this work, an uncontrolled bridge diode rectifier (Fig. 3), as shown in figure 1 (a), is utilized to convert the variable AC voltage of the

PMSG to variable DC voltage, by considering that the angles of switching and inductance are unimportant.

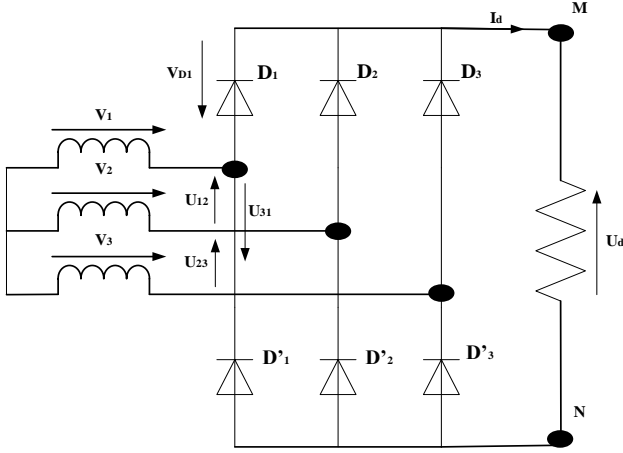


Fig. 3. Three phase bridge diode rectifier

The yield Current and voltage of the AC-DC converter are as follows [10]:

$$U_d = \frac{1}{T/2} \int_{-T/12}^{T/12} u_d dt = \frac{3\sqrt{6}}{\pi} \cdot U_{GSAP} \quad (9)$$

$$I_d = \frac{\pi}{6} I_{GSAP} \quad (10)$$

Where : U_d and I_d are the normal yield current and voltage values of the AC-DC converter, U_{GSAP} and I_{GSAP} are the operative voltage and current values of the alternative side.

d. DC-DC Boost Converter

The boost converter (figure 1(a)) steps up the input voltage to produce a higher output voltage. In addition, it plays a critical part in the entire WT framework operating as an interface between the bridge diode converter and the DC transport. This boost converter is hence utilized to extract the maximum available electric power from the wind generator. The schematic of the Boost converter power stage is given in the Figure below [13]:

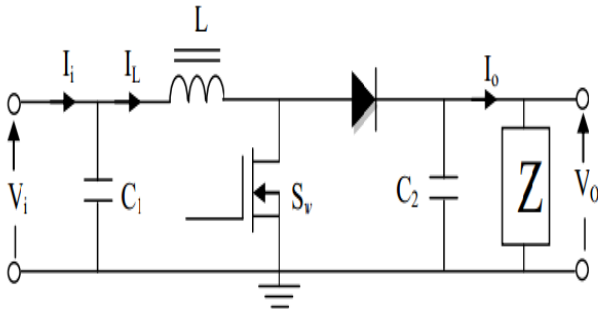


Fig. 4. DC-DC Boost converter model.

The dynamic model can be expressed by the following equations :

$$\begin{cases} \dot{V}_i = \frac{1}{C_1} (I_i - I_L) \\ I_L = \frac{1}{L} (V_i - (1 - D) \cdot V_0) \\ \dot{V}_0 = \frac{1}{C_2} (I_L - I_0) - \frac{D}{C_2} \cdot I_L \end{cases} \quad (11)$$

Where V_i : Input Voltage of the Buck Converter $D = 1$ when duty cycle is ON and $D = 0$ when duty cycle is OFF.

I_L : Inductor Current V_0 : output Voltage of the Boost converter; L : Inductance Value in Henry.

B) PV Generator Model

Various distinctions of the modeled PV exist in the literature, including the electrical circuit of the photovoltaic generator with two diodes as outlined in figure 5.

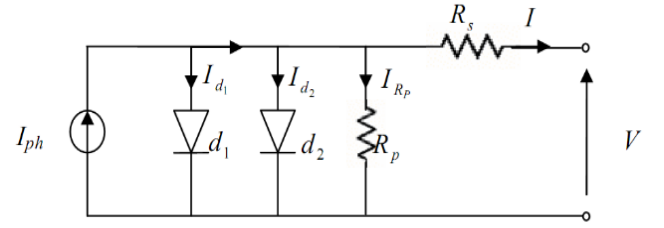


Fig. 5. Equivalent electrical graph of the two-diode model of a PV cell.

For modeling solar oriented illumination (Fig.5), a current source I_{ph} is utilized. The diodes d_1 and d_2 perform the polarization though the power misfortunes are individually illustrated by a series and parallel resistors R_s and R_p . The scientific model that portrays the PV panel comprising 36 cells connected in arrangement is given by :

$$I = I_{ph} - I_{S1} \left[\exp \left(\frac{q(V + I \cdot N_s \cdot R_s)}{N_s n_1 k T} \right) - 1 \right] - I_{S2} \left[\exp \left(\frac{q(V + I \cdot N_s \cdot R_s)}{N_s n_2 k T} \right) - 1 \right] - \frac{V + I \cdot N_s \cdot R_s}{N_s R_p} \quad (12)$$

I : PV module's terminal current (A)

$I_{ph} = S \cdot I_{ph,max}$: the photogenerated current (A) (where S is the irradiation)

V : PV module's voltage (V)

R_s : Series resistance (Ω)

R_p : Parallel resistance (Ω)

I_{S1}, I_{S2} : Diode's saturation currents (A)

n_1, n_2 : Ideality factors of diodes d_1 and d_2

N_s : Number of cells connected in series.

k : Boltzmann constant ($1.3806503 \cdot 10^{-23}$ J / K).

T : temperature (K)

q : Charge of the electron ($1.60217646 \text{ e-}19 \text{ C}$)

❖ MPPT for PV system

The PV framework employed in this research was operated under the most maximum power point tracking-MPPT- to extract the maximum available power from the panels, based on a Single Input Fuzzy Logic Controller (SIFLC). This latter employs error E as input and change in duty ratio dD as output. More subtle elements can be found in [14]. Taking $E = (\Delta P / \Delta V)$, for each step and by considering the sign of ΔP and ΔV , we conclude that :

$$\begin{aligned} \text{IF } E < 0 \text{ then } D &= D + \Delta D \\ \text{IF } E > 0 \text{ then } D &= D - \Delta D \\ \text{IF } E = 0 \text{ then } D &= D \end{aligned} \quad (13)$$

C) Model of Energy Storage System (ESS)

To maintain the DC link voltage at a desired value, a lead-acid battery and DC-DC bidirectional buck-boost converter were utilized. A model of this battery is displayed in figure 7:

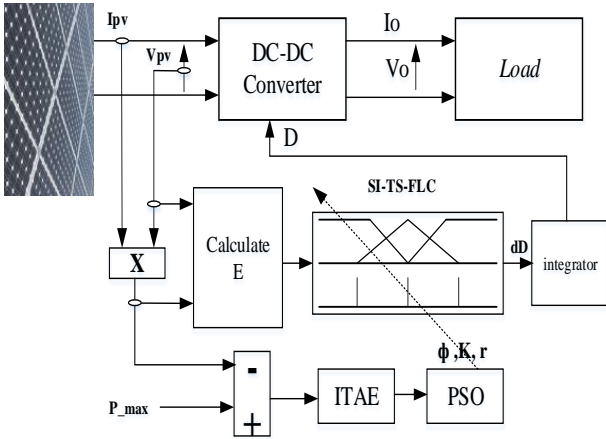


Fig.6. Block chart of a photovoltaic framework with SIFLC-MPPT method.

PSO algorithm is utilized for tuning FLC parameters (ϕ, k, r)

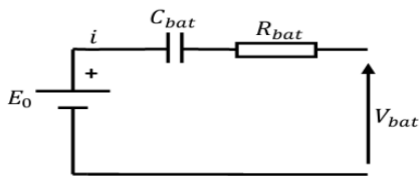


Fig.7. battery Model

The equation for measuring the battery voltage is as follows:

$$V_{batt} = E_o - iR_{in} - k \frac{Q}{Q - Q_{act}} + A \cdot \frac{Q - Q_{act}}{Q} \quad (14)$$

where:

E_o : Initial voltage, R_{in} : Internal resistance, i : Battery current, b_{batt} : Battery voltage,

A : Fitting constant, k : Fitting constant, Q : Nominal capacity et Q_{act} : Current battery capacity.

This model calculates the voltage over the battery, its state of charge (SOC) and losses. It is considered that the losses are simply ohmic resistors. To streamline the calculation, we put :

$$V_{batt} = E_o - iR_{in} \quad (15)$$

The battery SOC can be monitored using the following expression [18] :

$$\begin{aligned} \text{IF } E < 0 \text{ then } D &= D + \Delta D \\ \text{IF } E > 0 \text{ then } D &= D - \Delta D \\ \text{IF } E = 0 \text{ then } D &= D \end{aligned} \quad (16)$$

$$SOC = 100 \left(1 + \frac{\int idt}{Q} \right) \quad (17)$$

The battery charge-discharge depends on the available power, the request and the SOC [18-20].The power imperatives of the battery are decided based on the SOC limits :

$$SOC_{min} \leq SOC \leq SOC_{max} \quad (18)$$

The DC-link voltage is controlled within the ESS through a FOPID control methodology as shown in Fig. 8.

D) DC-AC Inverter Control

The DC-AC inverter portrayed in Figure 9 is utilized to supply the stack with consistent voltage in amplitude and frequency.

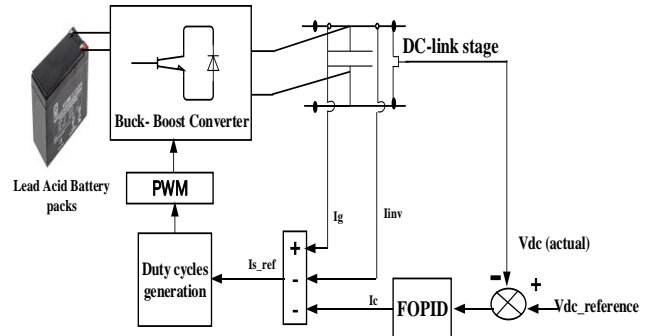


Fig. 8. ESS structure and control.

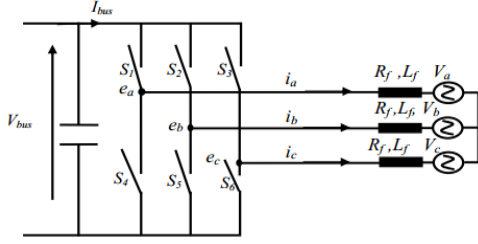


Fig. 9. Model of DC-AC inverter

The switches ($S_1, S_2, S_3, S_4, S_5,$ and S_6) have to be controlled in a complementary way to guarantee the coherence of substituting streams within the stack and to avoid, on the other hand, short circuit of the source. The vector of the straightforward voltages at the output of the inverter is composed of a matrix frame as follows [15] :

In the event that i_a, i_b, i_c are the currents of the alternative portion, the current within the continuous portion can be obtained from the power conservation law. Utilizing the expression ($P = V_{bus} \cdot I_{bus}$): where $f_1, f_2, f_3,$ are the switches states (On, Off). To control the line-to-line stack voltage; the authors apply voltage-fed control procedure. For more detailed elements, check references [9, 16, 17].

III. HYBRID ENERGY FRAMEWORK ADMINISTRATION

To oversee the electrical power produced by the HES (Fig. 1), we require an administrator, who must optimize the use of the delivered power and that of the battery. If renewable sources do not supply sufficient power while the battery capacity is adequate, which implies that the SOC is greater than the minimum value, the battery will provide the missing power (Fig. 10). Else, stack shedding is necessary to keep power adjusted, as the power supply is less than requested and the battery is at its minimum (SOCmin)[18, 19]; for our framework, it is supposed that the battery is completely charged at first. On the other hand, if the hybrid power exceeds the request of the stack, the excess will be stored in the battery and if this latter is full (SOC > SOCmax), the surplus will be dissipated in a dump stack (the resistance). In this way, the battery is not the main supplier; its charge / release rate is decreased, and hence, the battery life is extended, based on current commands of the different converters and on the estimation of the SOC of the batteries. Energy administration procedure flowchart updated in this consider can be displayed as follows :

$$\begin{bmatrix} e_a \\ e_b \\ e_c \end{bmatrix} = \frac{1}{3} V_{bus} \begin{bmatrix} 2 & -1 & -1 \\ -1 & 2 & -1 \\ -1 & -1 & 2 \end{bmatrix} \begin{bmatrix} f_1 \\ f_2 \\ f_3 \end{bmatrix} \quad (19)$$

$$I_{bus} = f_1(S_1, S_4) \cdot i_a + f_2(S_2, S_5) \cdot i_b + f_3(S_3, S_6) \cdot i_c \quad (20)$$

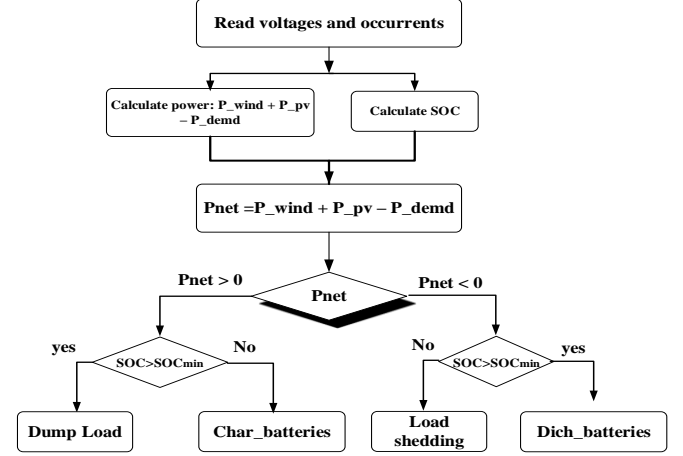


Fig. 10. HES Control administration flowchart

IV. RESULTS AND DISCUSSION

We assume that the state of charge of the battery is 85% (nearly full) to be able to check all operation cases. The requested control (P_{demd}), wind speed and illumination are variable to test the proposed controllers under different climatic conditions.

- For $t \in [0 \ 3s]$ (Fig. 11(a)), the demand power (P_{demd}) rises to ≈ 1400 W. It is given by the GPV since in this interval it produces ≈ 3360 W. (Fig. 11(c)), more than ≈ 1960 W compared to P_{demd} . The latter is stored in capacity batteries, which are then in charging mode, (Fig. 11.g).
- For $t \in [3 \ 5s]$ (Fig. 11(a)) the requested power attains ≈ 4700 W; which cannot be ensured by the two renewable sources (PV and wind). The power deficit ($P_{net} \approx 1550$ W) is provided by the batteries, which are then in release mode (Fig. 11(g)).
- At time 5 s, the wind turbine produces a power of ≈ 4300 W (Fig. 11(e)) which makes it conceivable to fulfill the power request and to charge the batteries at the same time at 7,5 seconds a drop of P_{demd} to nearly zero (Fig. 11(a)), the excess power becomes huge, which allows for charging the batteries.

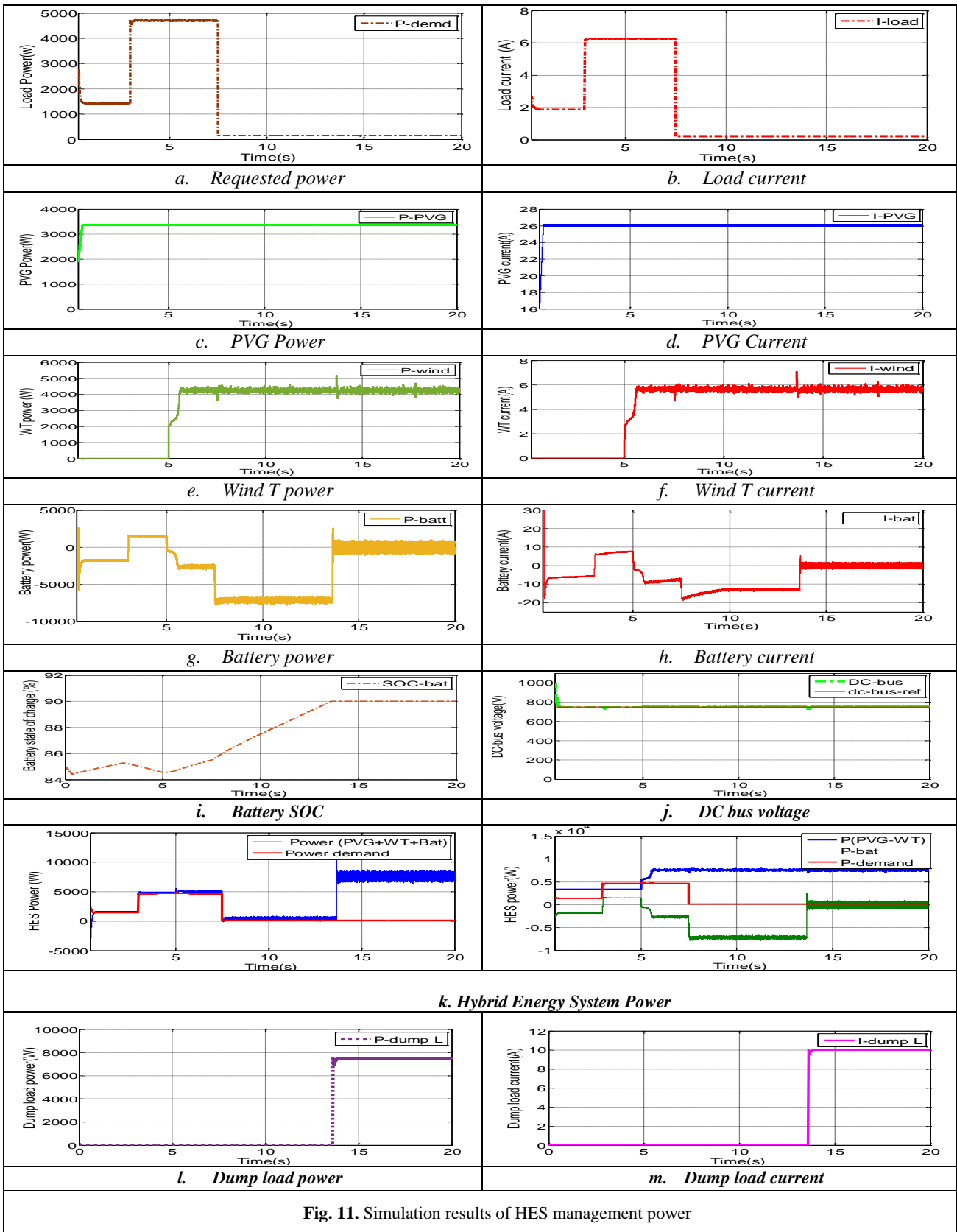


Fig. 11. Simulation results of HES management power

- At time 13.6s (Fig. 11(i)), the SOC attains its maximum value (90%). To prevent the battery from spilling, a dump stack is activated ($S1 = 1$) (Fig. 11(l)) to dissipate the power excess.
- Figure 11(j) shows the waveform of the DC bus voltage which is kept steady over the complete working range.

These simulations show that our controller offers good performance. It satisfies the stack request in spite of variation in climate conditions, while maintaining good control over the charging process of the battery.

V. CONCLUSION

An Energy administration control for a crossbreed wind PV with battery capacity is proposed in this paper to meet a stack request in any case of renewable sources intermittence or stack impedance variation. An MPPT controller for wind and solar array based on speed tracking and SIFLC respectively have been implemented to extract available wind and solar power. The line-to-line AC yield voltage control based on a PID controller, to supply the RL stack with steady sufficiency and recurrence was achieved. The adequacy of the proposed controls was assessed by using Matlab-Simulink. The obtained results show that the framework is very promising for future works.

VI. ACKNOWLEDGMENTS

The Authors greatly acknowledge the Algerian Ministry of Higher Education and Scientific Research

VII. APPENDIX

PMSG and Turbine Parametres	
pole Number (p)	14
stator resistance (R_s)	0.3676(Ω)
stator inductance (L_s)	0.00355
Magnetic flux (ϕ_f)	0.2867
Moment of Inertia (j+f)	7.856 Nm.rad/s
Turbine radius (r)	1.84
λ_{opt}	7.2
Cp_{opt}	0.38

- DC-DC converter parameters: $L=3.5\text{ mH}$, $C_1=C_2=5.6\text{ mF}$.
- PSO algorithm parameters: $c_1=c_2=2.05$ references

PVG Simulink model parameters	
Equivalent resistance in series : R_s (Ω)	15 $m\Omega$
Equivalent resistance in parallel: R_p (Ω)	30 Ω
Number of cells connected in series: N_s	36
Number of cells connected in parallel: N_p	1
Ideality factor of diode $d_1 :n_1$	1
Ideality factor of diode $d_2 :n_2$	2

VIII. REFERENCES

- [1] Renewables, Global Status Report,. (2018). REN21 (Renewable energy policy network for the 21st century). <http://www.ren21.net/status-of-renewables/global-status-report/>
- [2] L. Olatomiwa , S. Mekhilef , M.S. Ismail, M. Moghavvemi, *Energy management strategies in hybrid renewable energy systems : A review*, Renewable and Sustainable Energy Reviews vol. 62,PP. 821–835, 2016.
- [3] E. Dursun, and O. Kilic, *Comparative evaluation of different power management strategies of a stand-alone PV/wind/PEMFC hybrid power system*, Int J Electr Power Energy Syst; vol.34, N°1 PP.81–90, 2012.
- [4] D. Ipsakis, S. Voutetakis, P.Seferlis, F. Stergiopoulos, Papadopoulou S, Elmasides C., *The effect of the hysteresis band on power management strategies in a stand-alone power system*, Energy;vol.33,N°.10,PP.1537–50, 2008.
- [5] L. Blasques, JT. Pinho, *Metering systems and demand-side management models applied to hybrid renewable energy systems in micro-grid configuration*, Energy Policy; vol.45, PP.721–729, 2012.
- [6] B. Indu Rani, G. Saravana Ilango, C. Nagamani, *Control strategy for power flow management in a PV system supplying DC loads*, IEEE Trans Ind Electron; vol. 60, N°.8,PP.3185–94, 2013.
- [7] B. Benlahbib, F. Bouchafaa, N.Bouarroudj, S. Mekhilef, *Fractional Order PID Controller for DC link Voltage Regulation in Hybrid System Including Wind Turbine- and Battery packs- Experimental validation*, Int. J. Power Electronics, Vol.10, No.3, pp.289-313, 2019.
- [8] B. Benlahbib, and F. Bouchafaa, *PSO-PI algorithm for wind farm supervision*, Journal of Electrical Engineering, vol.14,N°. 3, pp.1–7, 2014.
- [9] Masmoudi, A., Krichen, L. & Ouali, A., *Voltage control of a variable speed wind turbine connected to an isolated load: Experimental study*, Energy Conversion and Management, 59, pp.19–26. 2012
- [10] A. Dahbi, M. Hachemi, N. Nait-said, *Realization and control of a wind turbine connected to the grid by using PMSG*, Energy Conversion and Management, vol. 84, pp.346–353, 2014.
- [11] M. Nasiri, , J. Milimonfared, S.H Fathi, *Modeling, analysis and comparison of TSR and OTC methods for MPPT and*

- power smoothing in permanent magnet synchronous generator-based wind turbines*, Energy Conversion and Management, vol. 86, PP.892–900, 2014.
- [12] B. Benlahbib, N. Bouarroudj, F. Bouchafaa, B. Batoun, *Fractional Order PI Controller for wind farm supervision*, 2014 IEEE International Conference on Industrial Engineering and Engineering Management, IEEE, pp. 1234–1238, 2014.
- [13] M. M. G. N., Kiran, Y. Parthasarthy, S., *Modelling of Buck DC-DC Converter Using Simulink*, International Journal of Innovative Research in Science, vol.3, N°. 7, PP.14965–14975, 2014.
- [14] B. Benlahbib, N. Bouarroudj, S. Mekhilef, T. Abdelkrim, A. Lakhdari, F. Bouchafaa, *A Fuzzy Logic Controller Based on Maximum Power Point Tracking Algorithm for Partially Shaded PV Array-Experimental Validation*, Elektronika ir Elektrotechnika, vol. 24, N°. 4, PP. 1392-1215, 2018.
- [15] A. Borni, et al., *P&O-PI and fuzzy-PI MPPT controllers and their time domain optimization using PSO and GA for grid-connected photovoltaic system: A comparative study*, International Journal of Power Electronics, vol.8, N°. 4, PP.300–322, 2017.
- [16] B. Benlahbib, et al., *Aerodynamic power forecasting in order to enhance wind farm supervision “ADRAR station in south Algeria*, Journal of Electrical Engineering, vol.15.N°. 4, PP.220–228, 2015.
- [17] B. Benlahbib, et al., *Wind farm management using artificial intelligent techniques*, International Journal of Electrical and Computer Engineering, vol. 7, N°. 3, PP.1133–1144, 2017.
- [18] B. Benlahbib, *Wind Farm Active and Reactive Power Management*, International Journal of Ambient Energy, 2020 DOI: 10.1080/01430750.2020.1861093.
- [19] Boualam Benlahbib, Nouredine Bouarroudj, Saad Mekhilef, Tameur Abdelkrim, Abdelkader Lakhdari, Farid Bouchafaa, *Power management and DC link voltage regulation in renewable energy system*, International Conference on Advanced Electrical Engineering (ICAEE)Algirs Algeria November, 19-21, 2019.
- [20] Boualam Benlahbib, Nouredine Bouarroudj, Saad Mekhilef, Dahbi Abdeldjalil, Tameur Abdelkrim, Farid Bouchafaa, Abdelkader Lakhdari, *Experimental investigation of power management and control of a PV/wind/fuel cell/battery hybrid energy system microgrid”* international journal of hydrogenenergy vol. 45 (53), PP :2 9110 -29122, 2020.